Chapter 13
A Feasibility Study of the Integration of Geologic CO_2 Storage with Enhanced Oil Recovery (CO_2 Flooding) in the Ordos Basin, China

Zunsheng Jiao, Ronald C. Surdam, Lifa Zhou and Yajun Wang

Abstract Rich in energy resources, China's Ordos Basin shares many similarities with Wyoming's Greater Green River Basin and Powder River Basin. As a result, the energy development strategy employed in Wyoming basins should be applicable to the Ordos Basin. The Ordos Basin's coal, coalbed methane, and natural gas reserves are ranked first in China, and its oil reserves are ranked fourth. The coal deposits in the Ordos Basin account for 39% (3.98 Tt) of Chinese coal resources, and six of the thirteen largest coal mines in China are in the basin. China's large energy base and the facilities essential to its fast-growing coal-to-chemicals industry are located in the Ordos Basin. The concurrent development of relatively new coal conversion industries with existing oil and gas industries in the Ordos Basin (Northern Shaanxi Province) provides the opportunity to apply the systematic approach to energy production developed in Wyoming: the integration of geologic CO_2 storage and enhanced oil recovery (EOR) using CO_2 flooding (CO_2-EOR). The coal conversion industry (coal-to-methanol, coal-to-olefins, etc.) provides affordable, capture-ready CO_2 sources for developing large-scale CO_2-EOR and carbon storage projects in the Ordos Basin. Compared with other CCUS projects, the ability to use CO_2 from the coal-conversion industry for CO_2-EOR and geologic CO_2 storage will make these projects in the Ordos Basin more cost-effective and technologically efficient while reducing CO_2 emissions to the atmosphere.

Z. Jiao (✉) · R. C. Surdam
Carbon Management Institute Laramie, University of Wyoming, Laramie, USA
e-mail: JJiao@uwyo.edu

R. C. Surdam
e-mail: rsurdam@uwyo.edu

L. Zhou · Y. Wang
Shaanxi Provincial Institute of Energy Resources and Chemical Engineering Xian, Shaanxi, P. R. China
e-mail: zhoulf@nwu.edu.cn

Y. Wang
e-mail: yajunwang@139.com

R. C. Surdam (ed.), *Geological CO_2 Storage Characterization,*
Springer Environmental Science and Engineering, DOI 10.1007/978-1-4614-5788-6_13,

The Shaanbei Slope of the Ordos Basin is a huge monoclinal structure with a high-priority potential CO_2 storage reservoir (Majiagou Formation) that lies beneath a sequence of Mesozoic rocks more than 2000 m thick containing a multitude of low-permeability lithologies. The targeted Ordovician Majiagou Formation in the area of interest is more than 700 m thick. This carbonate reservoir is located at depths where the pressure and temperatures are well above the supercritical point of CO_2. The targeted reservoir contains high-salinity brines (20,000–50,000 ppm TDS) that have little or no economic value. Preliminary simulation results show that the Ordovician Majiagou Formation in the Ordos Basin has excellent potential for geologic CO_2 sequestration and could store the CO_2 currently emitted by coal-to-chemicals facilities in Shaanxi Province for hundreds of years.

The extremely low porosity, low permeability, low oil saturation, anomalously low reservoir pressure, and high reservoir heterogeneity of the targeted CO_2-EOR formations in the Ordos Basin make using CO_2 for enhanced oil recovery much more challenging here than in the U.S. These reservoir characteristics together constitute a major reason that CO_2-EOR is not widely employed in the Ordos Basin at present, even though highly concentrated CO_2 from coal conversion plants has been available for years. Comparisons of reservoir and crude oil properties in the Ordos Basin with the current US CO_2-EOR screening guidelines reveal that the gravity, viscosity, crude oil composition, and formation type of the Ordos reservoirs all are favorable for CO_2 miscible flooding. The major challenges come from anomalously low reservoir pressure, low porosity, and higher reservoir heterogeneity.

13.1 Introduction

Rich in energy resources, China's Ordos Basin shares many similarities with Wyoming's Greater Green River and Powder River Basins. As a result, many elements of the energy development strategy developed for the Wyoming basins should prove directly applicable to the Ordos Basin. The Ordos Basin's coal, coalbed methane, and natural gas reserves rank first in China, and its oil reserves rank fourth. The coal deposits in the Ordos Basin account for 39 % (3.98 Tt) of total Chinese coal resources, and six of the thirteen largest coal mines in China are in the basin. China's largest energy base and the facilities essential to its fast-growing coal-to-chemicals industry are in the Ordos Basin. The coal conversion industry (coal-to-methanol, coal-to-olefins, etc.) will provide affordable, capture-ready CO_2 for large-scale CO_2-EOR and carbon storage projects in the Ordos Basin. The use of CO_2 from the coal-conversion industry for CO_2-EOR and geologic CO_2 storage in the Ordos Basin will make these EOR projects cost-effective and technologically efficient while reducing CO_2 emissions to the atmosphere.

Successful implementation of geologic CO_2 sequestration to manage carbon and mitigate climate change requires subsurface storage space for huge volumes of supercritical CO_2. A chosen storage formation must be capable of retaining the stored CO_2 for hundreds to thousands of years. A superior geologic storage site must pos-

sess three essential characteristics: adequate pore space, well connected pores, and a high-quality trapping mechanism. The Carbon Management Institute (CMI) at the University of Wyoming and the Shaanxi Provincial Institute of Energy Resources and Chemical Engineering (SPIERCE) have proposed that the Ordovician Majiagou Formation in the Ordos Basin is a superior potential geologic storage reservoir.

Furthermore, the concurrent development of relatively new coal conversion industries and existing oil and gas industries in the Ordos Basin has created a unique opportunity to apply the synergistic approach developed in Wyoming: the integration of geologic CO_2 storage and enhanced oil recovery using CO_2 flooding (CO_2-EOR). CO_2-EOR is a widely accepted and effective tertiary recovery technique that the oil industry has used for decades. In the United States, CO_2-EOR projects in Wyoming and Texas have demonstrated that CO_2-EOR can routinely increase oil recovery by 5–20%, depending on reservoir conditions and the applied technologies. With stranded oil recovery in a reservoir, about one-third of the injected CO_2 remains in the subsurface during the CO_2-EOR process, while about two-thirds is recycled and recompressed for injection back into the reservoir. By completion of production, the EOR project has created the significant potential for permanent CO_2 storage in the depleted reservoir. The integration of geologic CO_2 storage and enhanced oil recovery will increase oil and gas production, reduce CO_2 storage net expense and will improve environmental quality.

Applying experience gained from CO_2-EOR and CCS projects in Wyoming, researchers at the CMI are working closely with scientists from Northwest University, the Shaanxi Provincial Institute of Energy Resources and Chemical Engineering (SPIERCE), and the Yanchang Petroleum Company to expedite CO_2-EOR and geologic CO_2 storage projects in the Ordos Basin. At present, many CCS projects focus on CO_2 emitted by coal-fired power plants. High energy consumption penalties and the high cost of CO_2 capture from coal-fired power plants have become serious technical and financial obstacles for commercial-scale CCS and CO_2-EOR projects. In Northern Shaanxi Province, the coal conversion industies (coal-to-methanol, coal-to-olefins, etc.) provide affordable, capture-ready CO_2. Compared with other CCS projects, the use of CO_2 from the coal conversion industry for CO_2-EOR and geologic CO_2 storage will make these projects in the Ordos Basin more cost-effective and technologically efficient.

The geologic CO_2 storage capacity of the Majiagou Formation in the Ordos Basin has been assessed using high-resolution numerical simulation, as well as a volumetric approach. Presently, the mature oil fields in the Ordos Basin are being screened and prioritized on the basis of CO_2-EOR criteria and proximity to CO_2 sources (the coal conversion plants). Targeted high-priority candidates will be investigated further. Compared with the CO_2-EOR projects in the Texas and New Mexico Permian Basin and Wyoming Green River, Powder River, and Wind River Basins, the biggest challenge for CO_2-EOR projects in Northern Shaanxi Province is the development of advanced technology to deal with anomalously low-pressured reservoirs characterized by very low porosity and permeability and high reservoir heterogeneity. Three-dimensional reservoir characterization, CO_2-EOR potential screening, geologic storage reservoir modeling and injection numerical simulation,

systematic performance assessment, and economic evaluation will be used to select sites for a CO_2-EOR storage demonstration project in the Ordos Basin.

13.2 Geologic Setting

13.2.1 Geology

With an area of 370,000 km^2, the Ordos Basin (Fig. 13.1a) is the second largest sedimentary basin in China. The basin covers parts of Shaanxi, Shanxi, and Gansu provinces and the Ningxia and Inner Mongolia autonomous regions. Tectonically, the basin lies in the western North China Block and is bordered by the Luliang Mountains to the east, Qinling Mountains to the south, Liupan Mountains and Helan Mountains to the west, and Lang Mountains and Yin Mountains to the north. Separated by the Great Wall are the Maowusu and Kubuqi deserts to the north and the Loess Plateau to the south.

The Yellow River borders the Ordos Basin on the west, north, and east: all the water systems in the basin are part of the Yellow River drainage. Most watercourses in the desert and plain areas are intermittent streams that typically flow into desert lakes or salt marshes. Though its surface streams have small permanent flow and poor water quality, often drying out in summer, the Ordos Basin is rich in groundwater.

The Ordos Basin is a typical cratonic basin that developed into a large stable basin during the Paleozoic. The Shaanbei Slope with the exception of thrust fault features and depressions at the margins, the basin is a huge (110,000 km^2) monoclinal structure with a 1–2° west dip (Fig. 13.1b). The Shaanbei Slope is a relatively stable tectonic environment with rare regional faults, and is considered a favorable structural unit for geologic CO_2 storage.

The basement in the Ordos Basin consists of metamorphic Archean and Lower Proterozoic rocks. The basin has experienced five tectonic stages: (1) Middle to Late Proterozoic aulacogen, (2) Early Paleozoic shallow foreshore platform, (3) Late Paleozoic coastal plain, (4) Mesozoic inland basin, and (5) Cenozoic faulting depressions surrounding the basin. The Ordos Basin can be subdivided into six structural units: the Yimeng Uplift, Weibei Uplift, Jinxi Fault-Fold Belt, Shaanbei Slope, Tianhuan Depression, and Western Edge Fault Belt (Fig. 13.1a).

Sedimentary strata of the Proterozoic, Paleozoic, Mesozoic, and Cenozoic are extant in the Ordos Basin. The thickness of Paleozoic and Mesozoic sedimentary strata ranges from 2,559 to 7,847 m (Fig. 13.1c). From the Cambrian to the Early Ordovician, the Ordos Basin region was a shallow marine carbonate platform, and 300 to 600 m of carbonate rocks were deposited in the main part of the Ordos Basin. During the later Early Ordovician to Middle Ordovician, the North China Block (including the Ordos Basin) experienced a large-scale marine transgression that deposited 100–900 m of the Majiagou Formation, which consists of dolomite, lime-

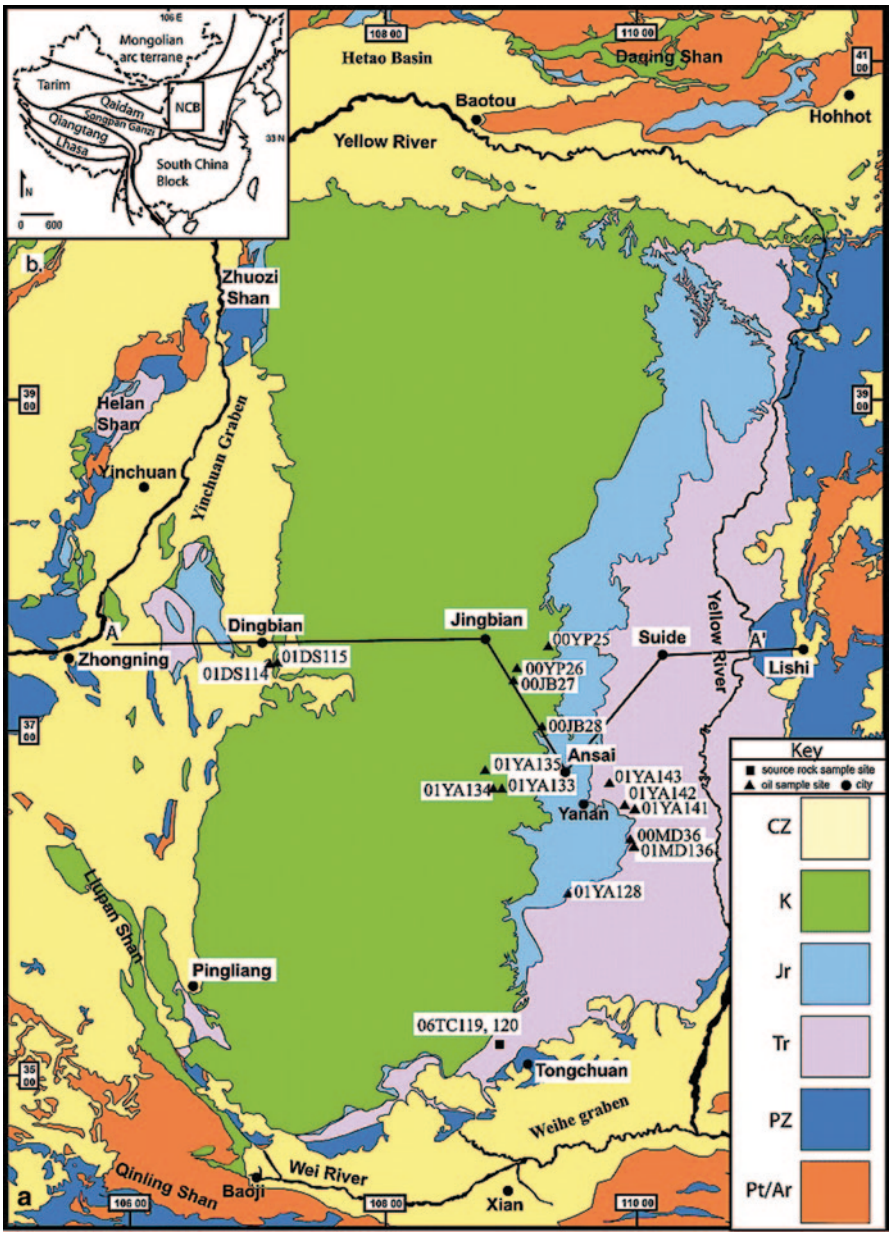

Fig. 13.1 (**a**) Geologic map of the Ordos Basin, China. (**b**) East-west geologic cross section of the Ordos Basin. (Modified from Li et al. 1989). (**c**) Stratigraphic column showing formation thickness, depositional environments, and reservoir and trap rocks in the Ordos Basin. (Modified from Yang et al. 2005)

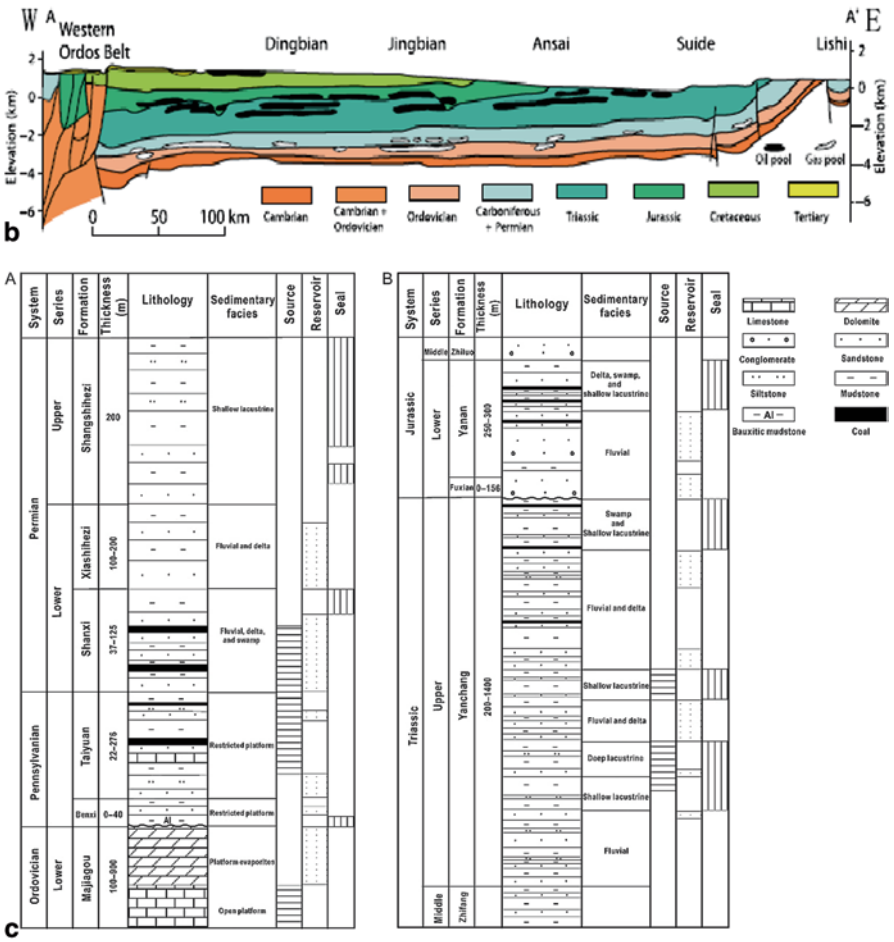

Fig. 13.1 (continued)

stone, and evaporitic rocks in the interior of the basin. Upper Ordovician, Silurian, Devonian, and Mississippian strata do not occur within the basin, and their absence is marked by a major regional unconformity between the Middle Ordovician and Pennsylvanian strata. During a 150 m.y. hiatus from the Middle Ordovician to the Mississippian, intense karstification of the Ordovician dolomites resulted in a wide distribution of karst strata along the regional unconformity forming the reservoir rocks of the Jingbian gas field. The average thickness of the upper Paleozoic sedimentary rocks ranges from 800 to 1000 m, mainly including the gas-bearing intervals of the Pennsylvanian Benxi Formation and the Permian Taiyuan, Shanxi, Shihezi, and Shiqianfeng formations. During the Triassic and Jurassic, a thick terrestrial stratigraphic section consisting of lacustrine, fluvial, wetland, and deltaic strata accumulated—comprising shales, mudstones, coal, and sandstones with a thickness

of 2300–5700 m. The Triassic Yanchang Formation is a major oil-rich unit in the Ordos Basin. During the Early Cretaceous, 100–1200 m of eolian sediments (eolian sandstones) were deposited in the Ordos Basin. In the Cenozoic, climate change brought drought to the Ordos Basin, and accompanied by uplift, the basin accumulated more than 200 m of wind-blown loess sediments.

The potential geologic CO_2 storage reservoirs in the Majiagou Formation lie beneath a 2000+ m thick sequence of Mesozoic rocks containing a multitude of low-permeability sealing lithologies. The Majiagou carbonate reservoir in the location of interest is more than 700 m thick and is located at depths where the pressure and temperature are well above the supercritical point of CO_2 (31 °C and 7.4 MPa). The targeted reservoir contains high-salinity brines (20,000–50,000 ppm) with no economic value at present. The Majiagou reservoir is continuous, as inferred from well logs and cores showing that porosity ranges from 1 to 15 % with average measured porosity of 8 % and that permeability ranges from 1 to 35 mD.

13.2.2 Oil, Gas, and Coal Resources

A major national energy and chemical industry development center, the Ordos Basin is the largest energy supplier in China, accounting for nearly 6, 13, and 39 % of national natural gas, coalbed methane, and coal reserves, respectively. The basin's crude oil reserves rank fourth in China. Oil, natural gas, coal, coalbed methane, and sandstone-type uranium are found in various tectonic structures and various sequences of Paleozoic to Mesozoic strata. While the oil reservoirs occur mainly in Triassic and Jurassic units in the southern basin, gas reservoirs occur predominantly in the northern basin in the Ordovician Majiagou Formation and Permian Shanxi and Shihezi formations (Figs. 13.1c and 13.2a). Coal resources are widely distributed in the Carboniferous, Permian, Jurassic, and Triassic stratigraphic section. The sandstone-type uranium deposits and coalbed methane are distributed mainly along the basin margins.

More than 40 oil fields have been discovered in the basin, including Xifeng field, the largest oil field found in the past 10 years, with reserves of 400 Mt of crude oil. Four of China's five largest gas fields, each with reserves of at least 100 Gm^3, are located in the Ordos Basin (Sulige, Jianbian, Wushenqi, and Yulin gas fields; Fig. 13.2a). The Ordos Basin contains more than 8 Gt of equivalent petroleum resources and about 11 Tm^3 of natural gas. In 2012, oil production from Petro China Changqing was 22.3 Mt and production from the Yanchang Group was 12.55 Mt: production from these two companies together is close to the total oil production of the Ordos Basin. Natural gas production in the Ordos Basin was 28.9 Gm^3, accounting for 25 % of China's 2012 gas production.

The Ordos Basin contains more than 39 % of China's coal resources, with resources of 3.98 Tt; of these resources, 2.41 Tt occur less than 1500 m deep. Coal production in the Ordos Basin was about 1.1 Gt in 2011; six of the thirteen major national coal mines are located in the Ordos Basin. The reserves of coalbed methane in the Ordos Basin are estimated to be at 7.8–11.3 Tm^3.

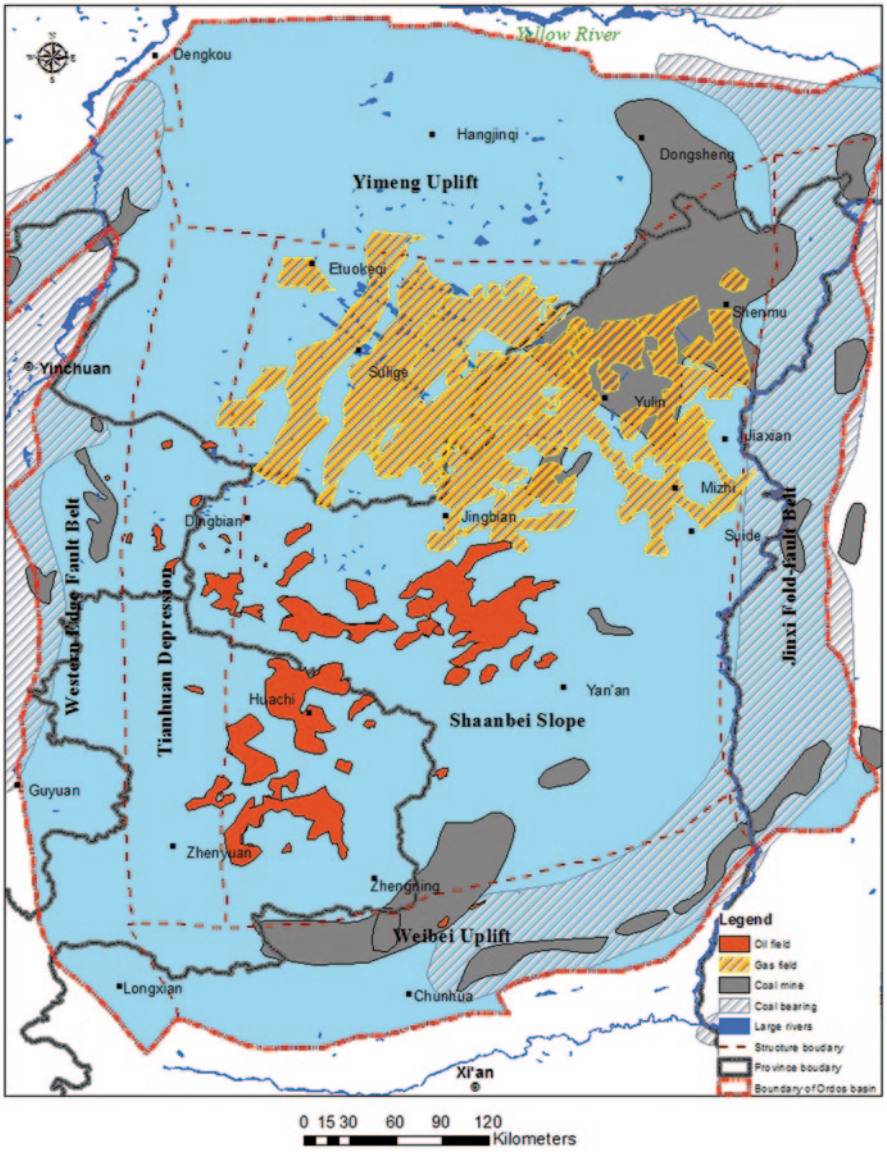

Fig. 13.2 (**a**) Map showing oil, gas, and coal fields in the Ordos Basin, and (**b**) map of large stationary CO_2 point sources designated by type and annual emissions in the Ordos Basin

13.2.3 Sources of Anthropogenic CO_2 in the Ordos Basin

Along with being China's number-one energy producer, the Ordos Basin also hosts the nation's largest coal-to-chemicals industry base. As more and more coal-fired power plants and coal-to-chemicals plants have been built near the coal mines in the Ordos Basin, anthropogenic CO_2 emissions have increased correspondingly and enormously.

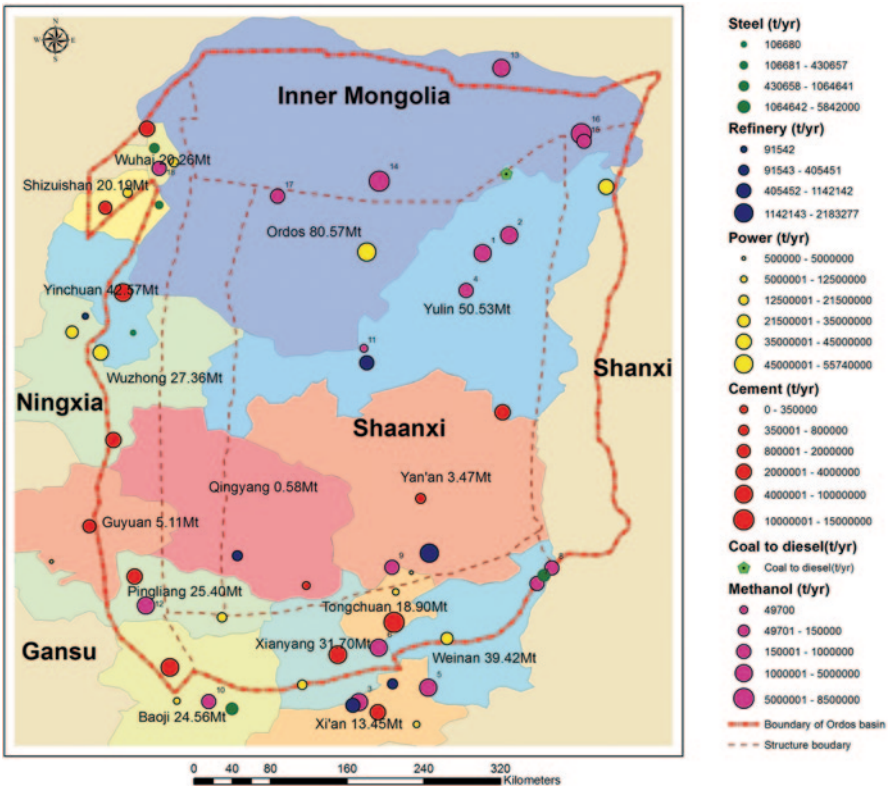

Fig. 13.2 (continued)

Industrial sectors examined within the scope of this study include coal-fired power plants, coal conversion plants (methanol, acetic acid, diesel, ethylene oxide), cement plants, iron and steel plants, petroleum refining facilities, and ammonia plants. The CO_2 emissions calculation methodology presented here is based on IPCC Guidelines for national greenhouse gas inventory and is based on available plant capacity and reported productivity. Total major anthropogenic CO_2 emissions ECO2 is given by:

$$ECO_2 = \sum_{j}^{n} \sum_{i}^{m} ECO_{2ji}, \tag{13.1}$$

where for recorded production

$$ECO_{2ji} = EF_{ji} \times P_{1ji},$$

and for production capacity

$$ECO_{2ji} = EF_{ji} \times P_{2ji} \times A_{ji} \times T_{ji},$$

Table 13.1 Estimated emission factors *EFji* for CO_2 emission sources (*i*) characterizing various industry sectors (*j*), in Kt of CO_2 per Kt of product, Kt of CO_2 per GWn for powerplants

Sector	CO_2 emission factor			
Cement(kt/kt)	0882[a]	0.867[b]	1.111[c]	1.102[d]
Power(kt/GWh)	1.000			
Iron & Steel(kt/kt)	1.270			
Refinery(kt/kt)	0.219			
Methanol(kt/kt)	5.67 ± 0.5			
Coal to diesel(kt/kt)	8.800			

[a] Dry process1; [b] Dry process2; [c] wet process1; [d] wet, process2

where ECO_{2ji} is the estimated annual CO_2 emissions from the *i*th emission source within the *j*th industry sector; EF_{ji} is the emission factor of the *i*th CO_2 emission source within the *j*th industry sector; $P1_{ji}$ is the production yield of the *i*th CO_2 emission source within the *j*th industry sector; $P2_{ji}$ is the production capacity of the *i*th CO_2 emission source within the *j*th industry sector; T_{ji} is the production rate, full load time (hours); *n* is the number of industry sectors *j*; and *m* is the number of emission sources *i* within sector *j*.

CO_2 emissions calculated for cement plants, refineries, iron and steel facilities, and ammonia plants are based on reported production, while production capacity was used for power plants and a mixture of production and production capacity for ethylene oxide and ethylene plants. Table 13.1 shows CO_2 emission factors for these sectors.

Figure 13.2b shows the stationary CO_2 sources in the Ordos Basin that emit at least 0.1 Mt of CO_2 per year. These sources comprise coal-to-chemicals plants, coal-fired power plants, refineries, cement plants, and ammonia and other chemical plants. Thus, this analysis does not consider all anthropogenic CO_2 emissions, and specifically does not include those from small industrial CO_2 point sources, transportation, direct energy use in commercial and residential buildings, land use, or agriculture.

More than 67 large stationary point sources in the Ordos Basin emit more than 0.1 M/year of CO_2. Annual CO_2 emissions from these sources total an estimated 409 Mt/year. Among these emissions are 44.02 Mt from methanol plants and 6.86 Mt from coal-to-diesel plants, giving 50.88 Mt of CO_2 per year emitted in high concentration (>95%), ready for capture, and ready for use for CO_2 flooding in the Ordos Basin.

13.3 Geologic Structural Modeling

We constructed a regional 3-D geologic structural model of the Ordos Basin utilizing well logs, isopach maps, and geologic data assembled from the literature. The model covers a major portion of the major Shaanbei Slope Block (420 × 750 km), and was built using the EarthVison® software, a 3-D geospatial modeling package. No faults are included in this geologic structural model. The model was generated around a 340×490×7-km 3-D grid matrix: the gridding on the X, Y, and Z axes

(width, length, and depth), 69×99×71, resulted in cells 5000 m wide, 5000 m long, and 100 m deep, respectively; 2-D and 3-D minimum-tension gridding was used. The 3-D geologic structural model was used to calculate the CO_2 storage capacity of the Majagou Formation using a volumetric approach.

A smaller 3-D geologic model, for a 50×50-km area centered near Hengshan city, was extracted from the regional geologic structural model. This smaller-scale model was used to generate a 3-D computational mesh for the Majiagou CO_2 injection simulation.

13.3.1 Generation of the 3-D Computational Mesh

Following the logic and methodology outlined by Miller et al. (2007), a 3-D computational hydrostratigraphic mesh was created from the smaller 50-km×50-km geologic structural model. In this computational mesh, the simulation cells or nodes were aligned to follow the curvature of the unit interfaces and do not stair-step in the manner of a traditional finite element grid. This allows more accurate calculation of CO_2 moving along the base of the caprock in the up-dip direction. This numerical mesh consists of a block 50-km×50-km in map view within the 340×490 km regional geologic structure model of the Shaanbei Slope Block, with elevation extending from 200 m above sea level to 3200 m below sea level. The grid spacing is 250 m in the X and Y directions at the injection area and increases logarithmically away from the injection area. The grid spacing in the Z (vertical) direction is 50 m in the injection interval and 100 m both above and below the injection interval. The total mesh comprises 320,000 nodes with 1.92 million volume elements (six volume elements per node).

13.3.2 CO_2 Injection Simulation Setups

Simulations of CO_2 injection were run on the Los Alamos National Laboratory Finite Element Heat and Mass Transfer (FEHM) multiphase porous flow simulator.

Initial conditions set for the model domain included a geothermal gradient of 26 °C/km with a domain bottom temperature of 135 °C and a domain top temperature of 47 °C, and a hydrostatic pressure ranging from 13 MPa at the top of the model domain 200 m above sea level to 44 MPa at the bottom of the modeling domain 3200 m below sea level. Further simplifying assumptions for the 3-D injection calculations were:

Rock thermal conductivity	0.5 W/mK
Rock density	2650 kg/m^3
Heat capacity	1000 J/kgK

Relative permeability for all rocks was assigned with a residual saturation of 10% for both brine and CO_2 using a linear relationship. Capillary pressure effects were ignored; brine TDS was assumed constant at 20,000 ppm for all formations, and water viscosity was calculated independently of brine content or dissolved CO_2. The initial dissolved CO_2 concentration was set to zero. During CO_2 injection simulation, the simulator accounted for CO_2 dissolution in water. For all simulations, the down-dip sides (west and south sides of the domain) were closed, whereas the up-dip sides (north and east sides) are open to reservoir fluid flow.

13.3.2.1 Majiagou Formation Simulations and Results

An important consideration in the CO_2 injection simulation scenarios is pressure buildup during injection. A limiting value of 75% of overburden pressure was selected for all simulations in order to ensure that the Majiagou Formation and overlaying sealing formations were not fractured during injection.

In order to evaluate the impacts of injection rate, porosity, and permeability on storage capacity, reservoir pressure evolution, and CO_2 plume migration trends, a series of CO_2 injection simulations was conducted with various combinations of injection rates and with various porosities and permeabilities for the targeted Majiagou Formation:

Injection rate	0.5, 1.0, 2.0 Mt/yr
Porosity	5, 10%
Permeability	1, 5 mD

All simulations used a formation thickness of 500 m (the actual thickness of the Majiagou Formation at the site is more than 700 m) within the 50×50×3.4-km numerical mesh block.

Three Majiagou simulations (with nine injection wells) with injection rates of 0.5, 1.0, and 2.0 Mt/year per well at a porosity of 10% and a permeability of 5 mD resulted in the storage of 4.5, 9, and 18 Mt/yr, respectively. These simulations were run for 100 years with CO_2 injection ending after the first 50 years (Fig. 13.3a). With an increase in the injection rate in the nine injection wells from 4.5 to 18 Mt/year, the maximum reservoir pressure increased from 40 to 55 MPa but remained below 60 MPa, 75% of the fracture pressure (80 MPa) of the Majiagou Formation in the study area. With greater CO_2 injection, the amount of fluid displaced also increased.

Figure 13.3b shows the results of three simulations with injection rates of 0.5, 1.0, and 2.0 Mt/year at a constant porosity of 5% and a permeability of 1 mD. Compared with the 10% porosity, 5 mD injection simulations (Fig. 13a), both the reservoir pressure and the volume of displaced fluid were greater with greater injection rate, but the magnitude of increase was much larger. With 1 mD permeability and at an injection rate of 18 Mt/year, (9 wells×2.0 Mt/year/well), the reservoir pressure reached 75% of the fracture pressure of the Majiagou Formation after 10 years of

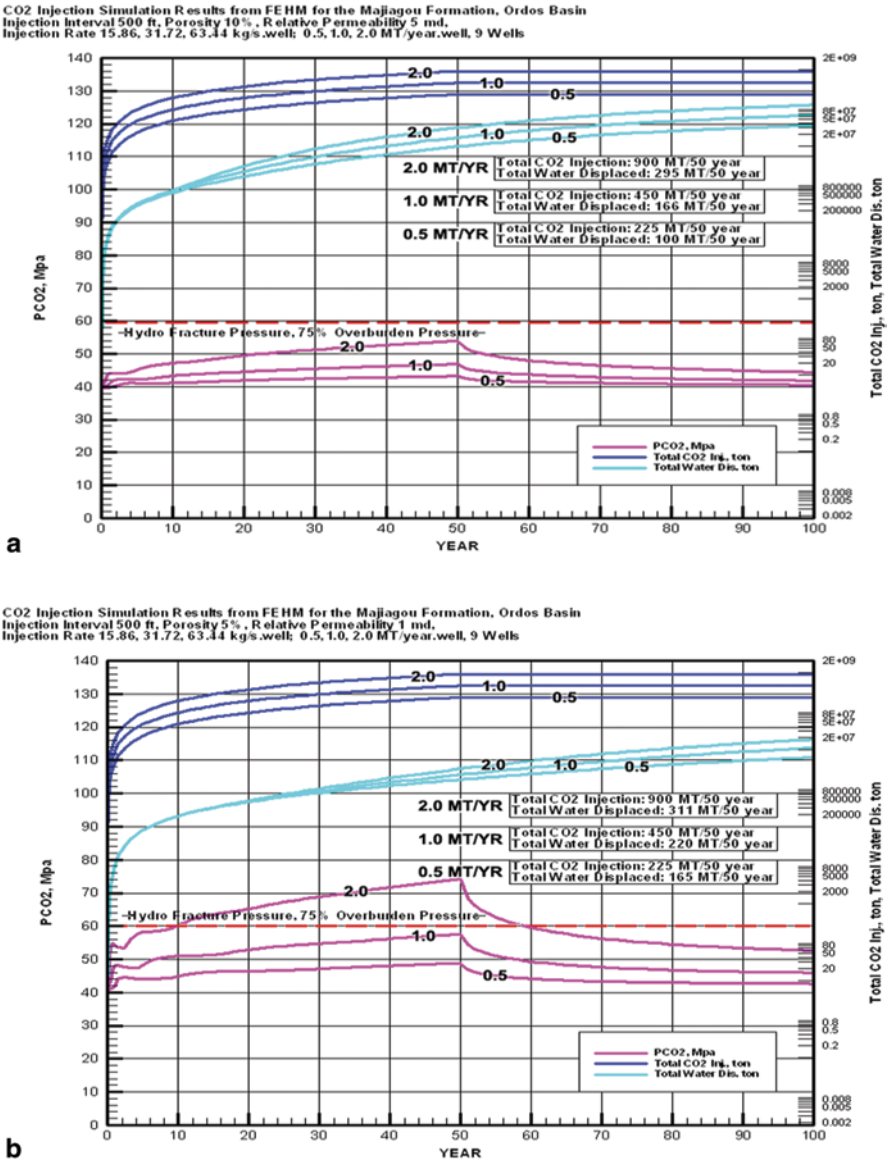

Fig. 13.3 FEHM simulation results for various porosities, permeabilities, and CO_2 injection rates. (From Jiao et al. 2011)

injection and kept increasing to near the lithostatic pressure. In all cases, the reservoir pressure dropped sharply when CO_2 injection stopped (Fig. 13.3a, b).

On the basis of all available measured data, an average porosity of 10% and a relative permeability of 5 mD for the Majiagou Formation were considered the most likely values for preliminary simulation. The input parameters for the most

reasonable simulation were a 1.0 Mt/year per well injection rate, 10 % porosity, and 5 mD permeability. With this set of parameters, results from the 50-year injection simulation show a total 450 Mt of CO_2 injected into the targeted reservoir and a total 166 Mt of original pore fluid displaced by the CO_2. Furthermore, the reservoir pressure remains well below the 75 %-of-fracture-pressure limit (Fig. 13.3a).

Simulation results suggest that saturation in the CO_2 plumes ranges from 0.1 to 0.9. The modeling results from this simulation showed that the CO_2 plume produced from a 1.0 Mt/year injection rate was relatively small after a total 450 million tonnes of CO_2 had been injected. The CO_2 plume remained within the 16 km × 15 km injection area after 50 years of CO_2 injection and stayed within an area of 17.7 km × 16 km after 100 years, 50 years post injection.

13.3.3 Storage Capacity Based on the Volumetric Approach

Burrus et al. (2009) present a method for estimating CO_2 storage capacity, the total known volume (TKV), based on the volume of pore space in a reservoir. The storage capacity in tonnes S_{TKV} [t] of a reservoir is given by:

$$S_{TKV} = T_a \times T_i \times N_{tp} \times \emptyset \times C_e \times C_f \times \rho_{CO_2}, \tag{13.2}$$

where T_a is the trap area [m^2]; T_i is the interval thickness of the storage formation [m]; N_{tp} is the fraction of T_i occupied by the reservoir interval [decimal fraction]; $\emptyset$ is the porosity [decimal fraction]; C_e is the storage efficiency factor (the fraction of the pore space that can be occupied by CO_2) [decimal fraction]; C_f is a unit conversion factor (here, $C_f = 1$); and ρ_{CO_2} is the density of CO_2 [t/m^3].

In order to use Eq. 13.2 to calculate the CO_2 storage capacity of the Majiagou Formation, the trap area (T_a) must first be defined. In other words, we must determine the upper and the lower depth limit of the targeted reservoir. The pressure and temperature required for CO_2 to be a stable supercritical fluid (31 °C and 7.4 MPa) are typically met at depths greater than 800 m (2600 ft) under a normal hydrostatic pressure gradient. To reduce the chance that the CO_2 would migrate to pressure and temperature conditions where it would change from the supercritical phase to liquid and vapor, a minimum storage depth of 1000 m (3,280 ft) was chosen for these estimates. The minimum storage depth sets the upper depth limit of a potential CO_2 reservoir. The choice of the lower depth limit for CO_2 storage is more arbitrary than that of the upper depth limit. It is based on the conclusion that if the CO_2 pressure at the wellhead is 15 MPa (2,175 psi) and CO_2 supercritical density is 0.65 g/cm^3, the CO_2 pressure will be 41 MPa (6000 psi) at the bottom of a 4000-m-deep (13,120 ft) well. Therefore, CO_2 injected at this depth will displace normally pressured formation water without additional compression. In the present study, 4 km (13,120 ft) is chosen for the maximum storage depth. On the assumption that 25 % of the formation thickness is available for storage the total volume of rock for CO_2 storage

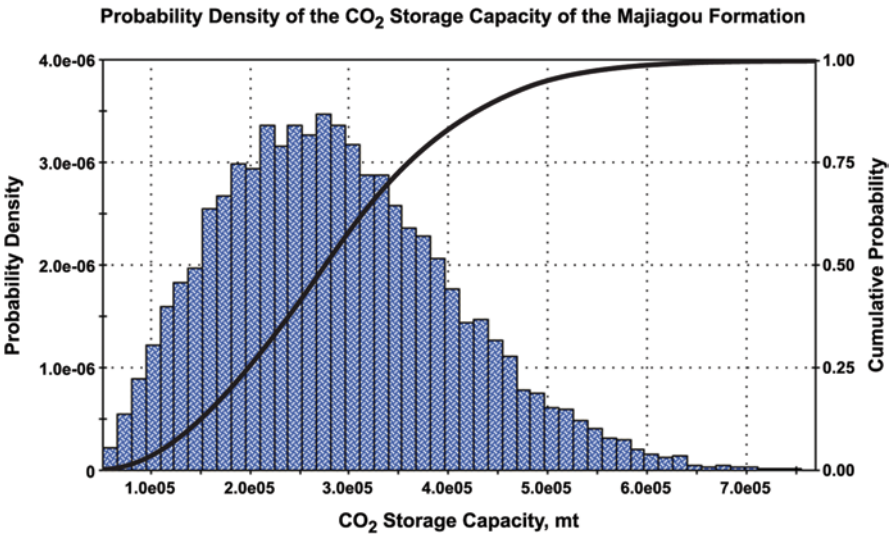

Fig. 13.4 Probability density of the CO_2 storage capacity in the Majiagou Formation, Ordos Basin. A cumulative probability of 25% yields a value of 200 Gt; this indicates that for this particular distribution, we have a 25% chance of storing 200 Gt of CO_2 or less. Put another way, this indicates that we have a 75% chance of storing at least 200 Gt CO_2 in the Majiagou Formation in the Ordos Basin

($T_a \times T_i \times N_{tp}$) was determined from the EarthVision® geologic structure model of the Majiagou Formation in the Ordos Basin to be 14,500 km^3.

A lognormal porosity distribution with a mean of 0.085, standard deviation 0.02, and skewness 0.44 was determined from all available Majiagou porosity measured data. For a saline aquifer, the upper limit on the storage efficiency factor *Ce* is related to the irreducible water saturation of the trap with CO_2 present. Values for irreducible water saturation in petroleum reservoirs are not well known, but probably range from a minimum of about 0.2 in gas reservoirs to about 0.6 in oil reservoirs. The results of the CO_2 injection simulation using FEHM show that most CO_2 saturation values range between 0.1 and 0.6. We chose a storage efficiency factor *Ce* for these simulations of 0.1 and 0.6.

A Monte Carlo simulation from Goldsim software with 10,000 realizations using the volume, porosity, and storage parameters described above was set up for the Majiagou Formation between depths of 1000 and 4000 m in the Shaanbei Slope of the Ordos Basin. Figure 13.4 shows the probability density of the CO_2 storage capacity of the Majiagou Formation in the Ordos Basin: ranges from 60 to 700 Gt, with a mean of 287 Gt (Fig. 13.4). Thus, the Majiagou Formation has sufficient storage capacity to accommodate decades of CO_2 emissions generated by the coal industry in the Ordos Basin.

13.4 Lessons Learned From Current U.S. CO_2-EOR Projects

Over the past 40 years, CO_2 flooding has become an established technology capable of effectively enhancing oil recovery in mature and mostly-depleted oil reservoirs. Particularly, CO_2 flooding improves the efficiency of oil recovery significantly compared with primary (pressure depletion) and secondary (water flooding) recovery methods (Oil and Gas Journal 2012, Manrique et al. 2010).

Production from 120 individual U.S. CO_2-EOR projects during 2012 averaged 352,221 barrels of oil per day (BOPD) (Oil and Gas Journal 2012), approximately 6% of the total U.S. crude oil production of about 6 million BOPD. Of the CO_2-EOR production, 308,564 BOPD was from CO_2 miscible flooding and 43,657 BOPD was from CO_2 immiscible flooding. CO_2 flooding technology has surpassed thermal technology (steam, in-situ combustion, and hot water) as the most commonly used method of tertiary enhanced oil recovery.

Miscible CO_2 flooding has achieved widespread use in the southwestern U.S., mainly in the Permian Basin, Rocky Mountains, and Mid-Continent region. There is additional EOR production in Alaska partly related to CO_2 injection. The oil and gas industry generally handles CO_2 in its supercritical phase, which is stable above the critical point, 6.9 MPa (1,087 psi) and 31 °C (88 °F). In its supercritical phase, injected CO_2 in the reservoir behaves like a liquid with respect to density and like a gas with respect to viscosity. Under suitable reservoir pressure and oil composition conditions, injected CO_2 mixes thoroughly with the crude oil within the reservoir, resulting in oil volume increase through oil swelling and a subsequent reduction of oil viscosity, eliminating interfacial tension between the oil and CO_2, and reducing the capillary forces that inhibit oil flow through the pores of the reservoir (Brock et al. 1989; Shtepani 2007; Manrique et al. 2012) Theoretically, all contacted oil could be recovered under CO_2 miscible flooding (Shtepani 2007), although in U.S. CO_2 flooding experience, recovery is usually limited to about 5–22% of the original oil in place. CO_2 flooding efficiency is affected by such parameters as reservoir residual pressure, residual oil saturation, oil composition and viscosity, reservoir porosity and permeability, sedimentary architecture, and especially reservoir heterogeneity and natural fractures.

On the basis of years of experience in the laboratory, field pilot and demonstration tests, and full-scale commercial operations, numerous miscible CO_2 enhanced oil recovery screening criteria have been suggested (Brashear and Kuuskraa 1978; Goodlett et al. 1986; Taber et al. 1997a, b; Klins 1984; Taber and Martin 1983; DOE 2010; Eduardo et al. 2008; Brock et al. 1989; Manrique et al. 2012). CO_2 flooding has been applied successfully in both sandstone and carbonate reservoirs. Homogenous, well connected, thin beds are preferred. For an optimal miscible CO_2 project, the crude oil specific gravity should be greater than 22° API; that of current projects ranges between 27° and 44° API. The recommended viscosity is less than 10 cp; that of current projects ranges from 0.3 to 6 cp. The residual oil saturation recommended is greater than 40%; the oil saturation of current projects range from 15 to 70%. A high percentage of intermediate composition in the crude oil (C5 to C12) is favorable for miscible CO_2 flooding. Residual reservoir pressure is a critical

parameter for a CO_2 flooding project. Many projects inject water to establish reservoir pressure before CO_2 flooding. The residual reservoir pressure must be greater than the minimum miscible pressure, which is generally determined by reservoir depth; the depth of existing projects ranges from 2500 ft to more than 11,250 ft (Peterson et al. 2012). Reservoir temperature is not a critical screening criterion, but higher temperatures increase the expandability of the crude oil. Porosity values vary widely among different depositional systems, but generally range between 6 and 30% (Beike and Holtz 1996). The type of porosity, as well as the amount, is important to EOR projects. Well-connected pores approaching uniform size are best for CO_2-EOR miscibility projects. Permeability determines the fluid dynamics of the reservoir. High permeability will allow large volumes of CO_2 to be injected into a single well, thus reducing cost. Homogenous high permeability will also allow CO_2 to move more quickly into a reservoir, increasing sweep efficiency.

Reservoir heterogeneity and natural fractures can contribute to an unsuccessful CO_2 flooding project, especially in a depositional system having high vertical and horizontal variability in permeability. Highly permeable strata can promote unstable flow (viscous fingering), resulting in early break-through of CO_2 and reduction of oil sweep efficiency. To prevent the occurrences of unstable flow and to reduce the amount of CO_2 consumed, CO_2 is typically injected into the reservoir alternately with water (WAG), because water sweeps through the reservoir more uniformly. WAG injection can significantly reduce viscous fingering and allow CO_2 flow through the reservoir after full miscibility is achieved.

13.5 An Integrated Energy/CCUS Development Strategy

The Carbon Management Institute at the University of Wyoming has created an integrated energy/CCUS development strategy to systematically and concurrently develop the coal mining and coal conversion industries, coalbed methane (CBM) production, CO_2 enhanced oil recovery, and CO_2 storage in the Powder River Basin, Wyoming. Chapter 12 is a full account of that integrated strategy.

The Ordos Basin geologic setting and energy resources profile are similar to those of the Powder River Basin. The concurrent development of new coal conversion industries and oil-and-gas industries in northern Shaanxi Province offers the opportunity for applying the integrated strategy developed in Wyoming: the integration of geologic CO_2 storage, and CO_2-EOR. The coal conversion industries (coal to methanol, coal to olefins, etc.) provide affordable, capture-ready CO_2 sources for large-scale CO_2-EOR and storage projects in the Ordos Basin. The ability to use CO_2 emitted by the coal-conversion industries for CO_2-EOR and geologic CO_2 storage will make these projects in the Ordos Basin cost-effective and technologically efficient.

An integrated energy development strategy has been developed for the Shaanbei National Energy Base. This integrated energy development strategy aims to synchronously, synergistically develop coal mining, the coal conversion industry,

coalbed methane production (CBM), CO_2 enhanced oil recovery, and CO_2 storage in the Shaanbei National Energy Base.

First, coal mining would continue using existing extractive technology or improved technology. Second, the new coal-to-chemicals facilities would be located as close to the coal mines as possible. In the Ordos Basin, recently constructed coal-to-chemicals plants are sited over underground coal mines (Shenmu Jinjie Industry Park and Yanchang Jinbian Industry Park). Third, coalbed-methane produced water would best support these coal conversion facilities. The volume of water required to supply the plants will vary. In the Ordos Basin, coal-to-methanol plant design is based on a 6:1 ratio of water to product. A 0.6-Mt methanol plant in the Ordos Basin annually uses 1.8 Mt of coal and 6.0 Mt of water, and emits 4.0 Mt of CO_2. A 7-million-barrels-per-year diesel plant annually uses 3.5 Mt of coal and approximately 56 Mt of water, and emits 2 Mt of CO_2. At present, the coal conversion industry in the Ordos Basin would generate 9.24 Mt of methanol and 0.78 Mt of diesel annually, and would emit 50.88 Mt of CO_2 in total. This readily captured, highly concentrated CO_2 would be stored in the adjacent depleted oil and gas fields or saline aquifers, such as Majiagou reservoirs, which have a tremendous CO_2 storage capacity. Furthermore, Liao et al. (2012) have assessed the CO_2 storage capacities of 14 depleted oil fields in the Ordos Basin at 100 Mt. These depleted oil fields are ideal (1) for storage of CO_2 emitted by coal conversion facilities and (2) as sources of CO_2 for EOR projects in adjacent depleted Yanchang reservoirs.

As shown in Fig. 13.2, more than 40 mature Yanchang oil fields with EOR potential are located near coal mining/conversion resource confluences, and are eligible for tertiary recovery via CO_2 flooding. Many have gone through the secondary recovery water flooding stage and appear ideal for CO_2 miscible flooding. These Yanchang oil fields together contained 2 Gt of original oil in place (OOIP) (Wang et al. 2007). Typically, CO_2 flooding could recover at least 10% additional production in the the Yanchang oil fields, 200 Mt of oil. Recovering the stranded oil via CO_2 flooding would require 700 Mt of CO_2 (3.5 t per tonne of incremental oil recovered). For a 30-year EOR project, about 23 Mt of CO_2 would be required annually. The current coal conversion facilities envisioned (50.88 Mt of CO_2 emitted annually) could more than adequately support theses EOR activities. A conservative estimate suggests that the CO_2 would be worth $40/t, or US$28 billion. Therefore, the CO_2 typically regarded as a problem with respect to sequestration would be worth approximately US$28 billion in this scenario. Moreover, the Yanchang reservoirs from which the stranded oil is recovered could be converted to permanent storage sites for CO_2, doubling the CO_2 storage capacity available to the coal conversion facilities.

13.6 CO_2 EOR Potential and Challenge in the Ordos asin

Most oil production in the Ordos Basin is from the Triassic Yanchang Formation (Fig. 13.1c). The interbedded lenticular sandstone, siltstone, mudstone, and shale accumulated in fluvial, delta, and lacustrine depositional environments. The Tri-

assic Yanchang reservoirs have extremely low porosity, low permeability, low oil saturation, anomalously low reservoir pressure, and great heterogeneity. These characteristics have directly resulted in very low primary and secondary recovery, less than 15% in most oil fields in the basin. Table 13.2 shows reservoir and crude oil properties for selected Yanchang reservoirs.

The depth of Yanchang reservoirs in the Ordos Basin ranges from 150 to 2200 m. The individual sandstone beds range in thickness from 7 to 15 m. The porosities range from 8 to 17%. Permeabilities range from 0.5 to 38 mD, and many are less than 1 mD. The formation water type is calcium chloride with total dissolved solid from 10,000 to 70,000 ppm. The reservoir is regionally underpressured, even at the beginning of field development. The crude oil is light or intermediate, with specific gravity ranging from 0.72 to 0.84 or 35 to 62° API. Most of the reservoirs have oil saturations from 40 to 60%. Because all reservoir sandstones were deposited in fluvial and lacustrine environments, very low continuity and high heterogeneity is common in most reservoirs. Multi-age natural fractures are found in most cores from the Yanchang reservoirs.

A typical distribution of the Yanchang pay zones in an Ordos Basin reservoir shows compartmentalized, disconnected, lenticular sandstone and siltstone pay zones separated by mudstones and shales. Multiple fracture systems compound the reservoir heterogeneity.

Low porosity, low permeability, low oil saturation, anomalously low pressure, and high reservoir heterogeneity make using CO_2 enhanced oil recovery more challengeing than any CO_2 EOR project in the United States. This is a major reason that CO_2 EOR has not been widely developed in the Ordos Basin, even though CO_2 sources have been available for years. Table 13.2 lists reservoir and crude oil properties for selected oil reservoirs in the Ordos Basin. The depth of the reservoirs ranges from 200 to 2200 m. The individual bed thickness in the pay zone ranges from 5 to 18 m. The crude oil is light oil or intermediate oil with specific gravity ranging from 0.73 to 0.86 (33 to 62° API) and viscosity ranging from 1.3 to 9 mPas. All Yanchang reservoirs are anomalously underpressured, with a pressure coefficient of 0.9 (0.39 psi/ft). Therefore, the residual pressure in most candidate reservoirs is below the minimum miscible pressure. Most reservoirs are characterized by low porosity and permeability. The porosity for selected reservoirs ranges from 8 to 17%, and permeability from 0.5 to 38 mD.

Table 13.3 compares Ordos reservoir and crude oil properties with current U.S. CO_2-EOR screening guidelines and practice (Taber et al. 1997; Shtepani 2007; Lake et al. 2008). In this comparison gravity, viscosity, crude oil composition, oil saturation, and formation type of the Ordos reservoirs are favorable for CO_2 miscible flooding. The major challenge results from the anomalously low reservoir pressure, low porosity, and greater reservoir heterogeneity. The low permeability may help to increase CO_2-oil multiple contact chances but may hinder attainment of sufficient flow rates.

Even though a CO_2-EOR project in the Ordos Basin faces challenges, Ordos has many favorable characteristics for developing CO_2-EOR technology. Besides available local CO_2 sources, the thin beds and compartmentalized reservoirs are

Table 13.2 Reservoir and crude oil properties for selected oil reservois in the Ordos Basin, China

Oil field	Depth meter	Reservoir	Bed Thinck. (m)	Specific Gravity	API	Viscosity (mPa.s)	Pressure (Mpa)	Temp. (°C)	Porosity (%)	Perm. (md)	Oil Satura (%)	TDS (mg/l)	MMP[1](Mpa)
YC	200–250	Chang 6	13	0.84	37	4.9	1.8	19	9.9	0.55		10,000	
YP	400–450	Chang 2	7.6	0.85	35	5.5	3.6	23	13	6.5		46,000	
ZC	400–450	Chang 6	7.6	0.84	37	5.5	3.6	23	11.2	1.65	53.6	42,400–87,600	
QH	400–450	Chang 2	8.7	0.84	37	6.3	3.6	23	14	15			
YD	350–550	Chang 6	15.7	0.84	37	6.3	4	24	9.4	0.5	51		
GG	150–350	Chang 6	16	0.83	39	3.9	2	20	9.5	0.54	50.3	10,000	
ZY	150–350	Chang 6	14.5	0.85	35	3.5	2	20	9.2	0.3	56		
ZL	600–800	Chang 2	5–18	0.85	35	8.9	7	32	17	7.3	42	50,000–70,000	
TJ	600	Chang 2	14.8	0.84	37	4.6		29	17.6	38.2			
PQ	1,000	Chang 2, 4+5, 6	9.9	0.86	33	4.45–7.83	9	41	11	2.8	55		
QY	1,000	Chang 6	12	0.84	37	3.92	9	41	13.5	1.6	55.6		
HS	1,100	Chang 6	9.8	0.845	36	5.42	10	44	13.7	2.5	56		
XH	1,200	Chang 6	6.7	0.85	35	5	11	47	12	2.5			
HU	1,800		12	0.77	52	1.64	18	71.6	10	0.5			19.5
MU	2,200		14	0.73	62	1.35	22	76	8	0.5			19.8
DB	2,000	12 Chang 6	0.78	50	2	12	44	8	1	40	70,000	15.7	

All crude oil is light/intermediate type. All watert is $CaCl_2$

[1] Minimum miscibility pressure

Table 13.3 Comparison of Ordos reservoir/crude oil properties with the US CO_2 EOR screening Guidline

	US Recommended	US Current Projects Rang	Ordos
Gravity	<0.92 (>22 API)	0.81–0.89 (27–44 API)	0.73–0.86 (33–62 API)
Viscosity	<10 cp	0.3–6	1.3–9 cp
Composition	High C5 to C12 percent light -intermediates		Light-intermediates
Oil Saturation	>40%	15–70%	40–56
Formation	Thin beds	Sandstone/carbonate	Thin sandstone beds
Porosity	>8%	4–18%	5–17%
Per me ability	Not critical	3–31 md	0.1–7 md
Depth	>800 m (2,600 ft)		200–2500 m (650–8200 ft)

favorable for creating a stable flow (reducing CO_2 flow fingering) and increasing sweep efficiency. Reservoir pressure is one of the most important factors of CO_2 miscibility in oil. According to Klins and Bardon (1991) and Shtepani et al. (2007), it is possible to achieve a different level of miscibilities, ranging from immiscible (low-pressure reservoirs) through intermediate- to high-pressure applications (miscible displacement). The minimum miscibility pressure has a wide range of values depending on depth, temperature, and crude oil composition. A minimum of 8 MPa (1,160 psi) is generally regarded as a target reservoir pressure at which to conduct a successful CO_2 flood. This condition imposes an important restriction related to the current level of reservoir pressure for miscible CO_2 flooding. A significant number of reservoirs in the Ordos Basin fall below this level (Fig. 13.5).

Figure 13.5 shows oil fields superimposed on a map of the burial depth of the Yanchang Formation, the main oil and gas producing formation in the Ordos Basin. The heavy black line is the 800 m contour of the burial depth of the top of Yanchang Formation. The depths of oil fields that fall inside the heavy black line are below 800 m depth. Because the oil and gas reservoirs in the Ordos Basin typically have a very low content of movable formation water, water flooding is not efficient for secondary oil recovery. Injecting CO_2 into a reservoir before oil production could be an efficient way to establish reservoir pressures that meet the minimum miscible pressure requirement.

A pre-CO_2 injection simulation for building reservoir pressure was generated for a different scenario. For the test reservoir, the average depth of the targeted reservoir is 1500 m, porosity is 10%, and permeability is 1 mD. The injection rate of supercritical CO_2 is 23 kg/min. The depleted reservoir is anomalously underpressured at 11.5 MPa. The simulation results from the Los Alamos National Laboratory FEHM simulator shows that minimum miscible pressure could be established for this reservoir after 100 days of supercritical CO_2 injection (Fig. 13.6).

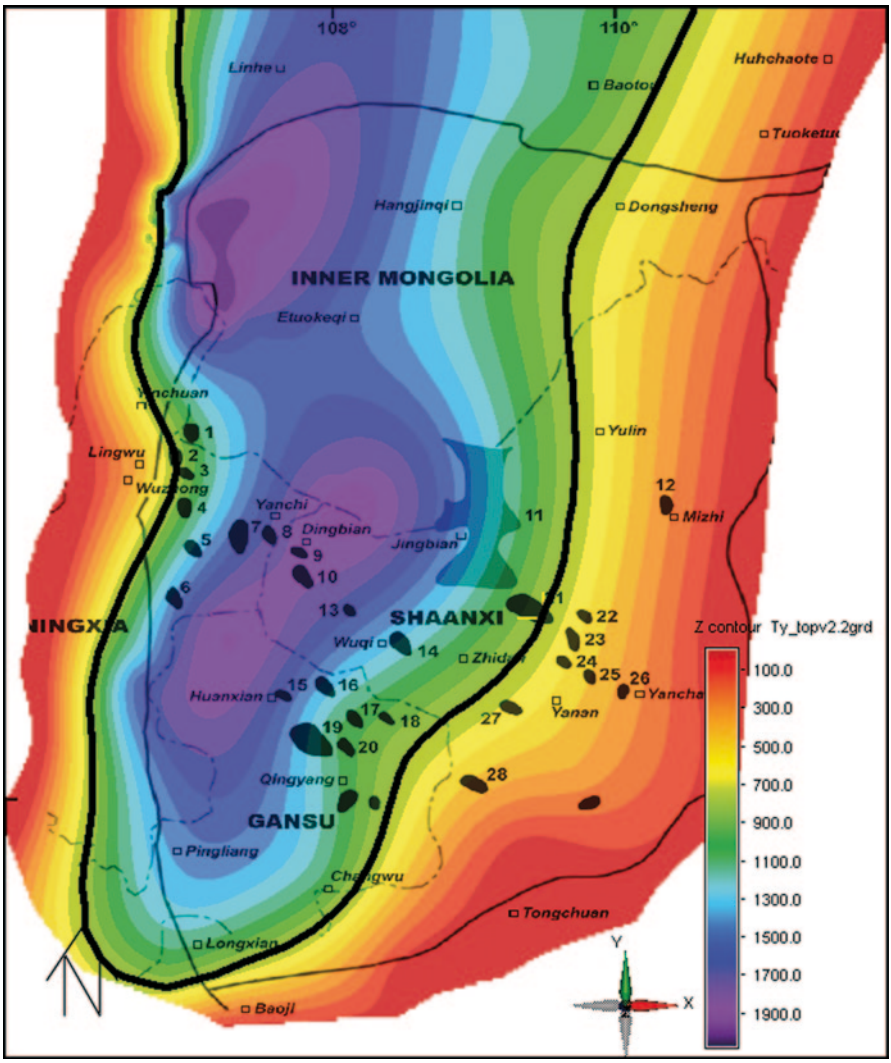

Fig. 13.5 Yanchang Formation oil fields superimposed on a map of the burial depth of the Yanchang Formation top

References

Brashear JP, Kuuskraa VA (1978) The potential and economics of enhanced oil Recovery. J Petrol Technol. SPE paper 6350

Brock W, Bryan L (1989) Summery results of CO_2 EOR field tests, 1972–1987. SPE paper 18977

Goodlett G (1986) Lab evaluation requires appropriate techniques. Oil Gas J June:23

Jiao Z, Surdam RC, Zhou L, Stauffer P (2011) A feasibility study of geological CO_2 sequestration in the Ordos Basin. Energy Procedia 4:5982–5989

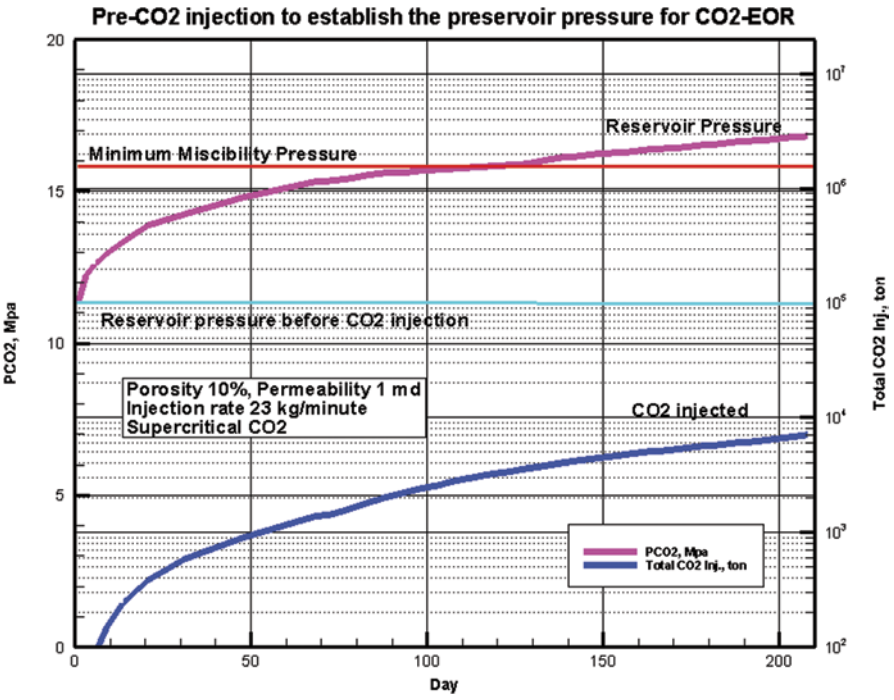

Fig. 13.6 Plot of the results of the CO_2 injection simulation from the LANL FEHM simulator showing injection rate and time needed to establish the minimum miscible pressure for a miscible CO_2 flooding project

Klins MA (1984) Carbon dioxide flooding, basic mechanisms and project design. International Human Resources Development Corporation, Boston

Klins MA, Bardon CP (1991) Carbon dioxide flooding. Institut Francais du Pétrole

Koottungal L (2012) 2012 worldwide EOR survey. Oil Gas J April:2

Kuuskraa V, Ferguson R (2008) Storage CO_2 with enhanced oil recovery. DOE/NETL 402/1312/02-07-08

Lake L, Walsh M (2008) Enhanced oil recovery (EOR) field data, literature search. University of Texas at Austin

Marique E, Izadi CM, Lantz M, Alvarado V (2008) Effective EOR decision strategies with limited data: field cases demonstration. SPE paper 113269

Marique E, Thomas C, Ravikiran R, Izadi M, Lantz M, Romero J, and Alvarado V (2010) EOR: current status and opportumities. SPE paper 130113

Meyer J (2008) Summary of carbon dioxide enhanced oil recovery (CO_2-EOR) injection well technology. American Petroleum Institute

National Energy Technology Laboratory (NRTL) (DOE) (2010) Carbon dioxide enhanced oil recovery. www.netl.doe.gov

Peterson C, Pearson E, Chodur V, Periera C (2012) Beaver Creek Madison CO_2 enhanced oil recovery project case study, Riverton, Wyoming. SPE paper 152862

Shtepani E (2007) Experimental and modeling requirements for compositional simulation of miscible CO_2-EOR processes. SPE paper 111290

Surdam R, Jiao Z, Bentley R, Ganshin Y, Heller P, Fan M, DeBruin R, Rodgers J (2011) CO_2 sequestration in depleted compartmentalized gas fields—the key to deploying clean coal technology in the Powder River Basin, Wyoming. University of Wyoming School of Energy Resources, Laramie

Taber JJ, Martin FD (1983) Technical screening guides for the enhanced recovery of oil. SPE paper 12069

Taber JJ, Martin FD, Seright RS (1997a) EOR Screening criteria revisited—Part 1: Introduction to screening criteria and enhanced recovery field projects. SPE paper 35385

Taber JJ, Martin FD, Seright RS (1997b) EOR screening criteria revisited—Part 2: Application and impact on oil prices. SPERE Aug:199–205

Yang Y, Li W, Ma L (2005) Tectonic and stratigraphic controls of hydrocarbon systems in the Ordos Basin: a multicycle cratonic basin in the central China, AAPG Bull 89(2):255–269